Supporting information

Nitrogen-doped carbon layer coated Co(OH)F/CoP_2 nanosheets for high-current hydrogen evolution reaction in alkaline freshwater and seawater

Yuxuan Wang[1], Chao Fan[1], Kang Wang, and Yan-Qin Wang*

Inner Mongolia Key Laboratory of Chemistry and Physics of Rare Earth Materials, College of Chemistry and Chemical Engineering, Inner Mongolia University, 24 Zhaojun Road, Hohhot 010021, P. R. China

E-mail: yqwang_chem@imu.edu.cn

[1]Yuxuan Wang and Chao Fan contributed equally.

1. Supporting Figures and Table

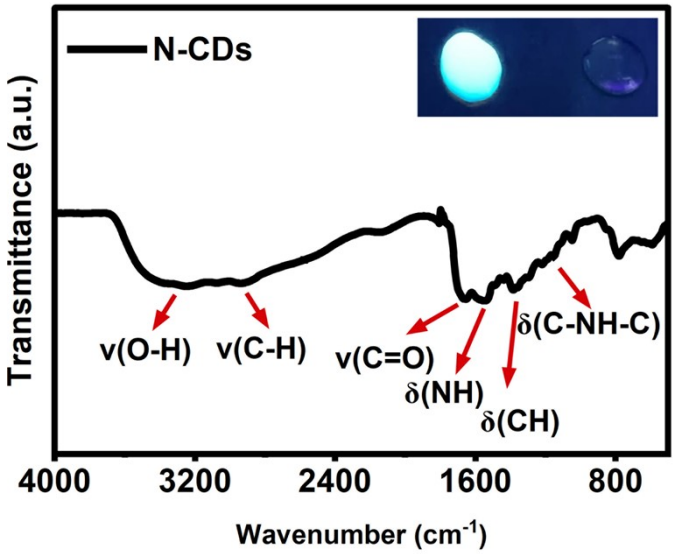

Fig. S1 FTIR spectra of N-CDs, the inset is the picture of N-CDs solution and deionized water under UV light irradiation.

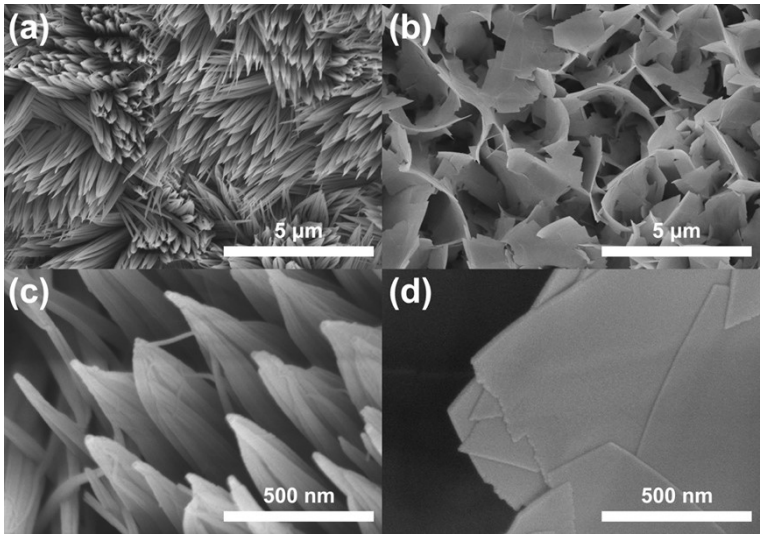

Fig. S2 SEM images of catalysts at different magnifications. (a, c) Co(OH)F/Co(OH)$(CO_3)_{0.5}$/NF, and (b, d) NC@Co(OH)F/Co(OH)$(CO_3)_{0.5}$/NF.

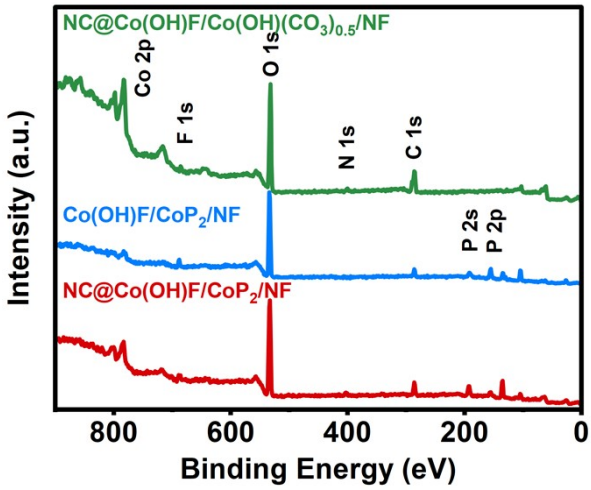

Fig. S3 The survey XPS spectra of NC@Co(OH)F/Co(OH)$(CO_3)_{0.5}$/NF, Co(OH)F/CoP_2/NF, and NC@Co(OH)F/CoP_2/NF.

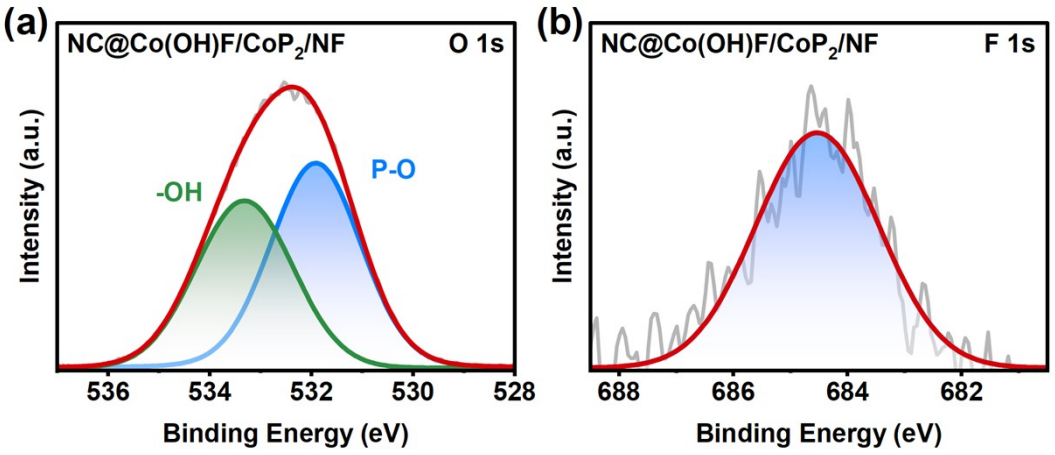

Fig. S4 XPS spectra for (a) O 1s, and (b) F 1s of NC@Co(OH)F/CoP_2/NF.

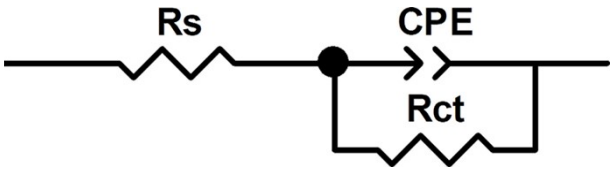

Fig. S5 The one-time-constant model equivalent circuit used for data fitting of EIS spectra (R_s is the overall series resistance, CPE is the constant-phase element, and R_{ct} is the charge transfer resistance related to HER processes).

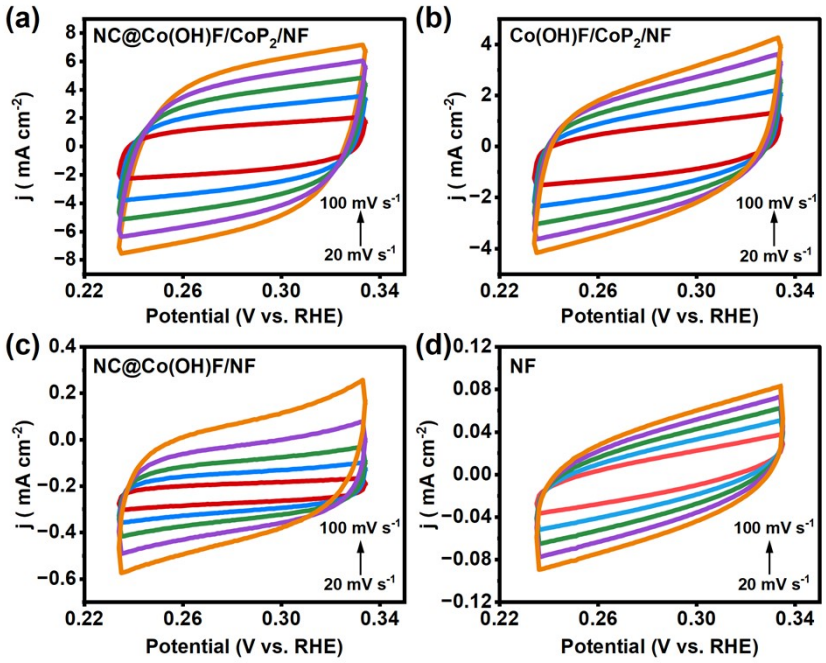

Fig. S6 Cyclic voltammograms at various scan rates in the potential range of 0.22 ~ 0.33 V vs. RHE for NC@Co(OH)F/CoP_2/NF (a), Co(OH)F/CoP_2/NF (b), NC@Co(OH)F/NF (c) and NF (d), respectively.

The ECSA was determined assuming a general specific C_{dl} capacitance of 40 μF cm^{-2}. For all samples, the ECSA is estimated by the following formula:

$$A_{ECSA} = \frac{Specific\ capacitance\ (\mu F\ cm^{-2})}{40\ \mu F\ cm^{-2}\ per\ cm^{2}_{ECSA}}$$

$$A^{NC@Co(OH)F/CoP_2/NF}_{ECSA} = \frac{50.96\ mF\ cm^{2}}{40\ \mu F\ cm^{-2}\ per\ cm^{2}_{ECSA}} = 1274\ cm^{2}_{ECSA}$$

$$A_{ECSA}^{Co(OH)F/CoP_2/NF} = \frac{22.75\ mF\ cm^2}{40\ \mu F\ cm^{-2}\ per\ cm_{ECSA}^2} = 568.75\ cm_{ECSA}^2$$

$$A_{ECSA}^{NC@Co(OH)F/NF} = \frac{2.60\ mF\ cm^2}{40\ \mu F\ cm^{-2}\ per\ cm_{ECSA}^2} = 65\ cm_{ECSA}^2$$

$$A_{ECSA}^{NF} = \frac{0.45\ mF\ cm^2}{40\ \mu F\ cm^{-2}\ per\ cm_{ECSA}^2} = 11.25\ cm_{ECSA}^2$$

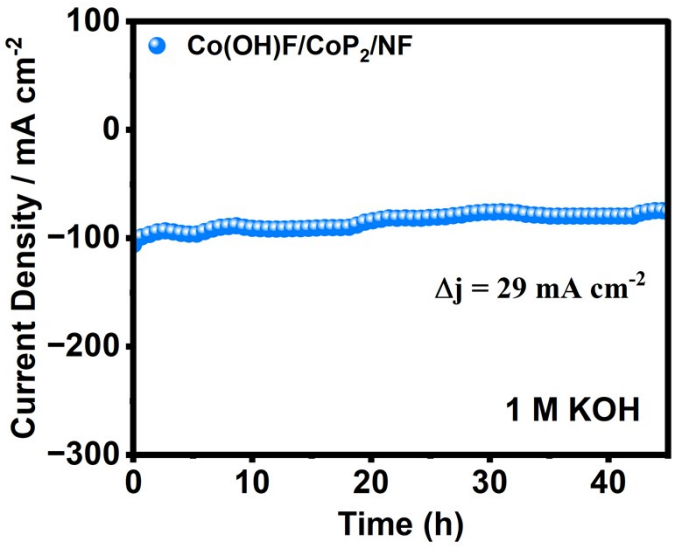

Fig. S7 The i-t test of Co(OH)F/CoP_2/NF at 100 mA cm^{-2} in 1.0 M KOH.

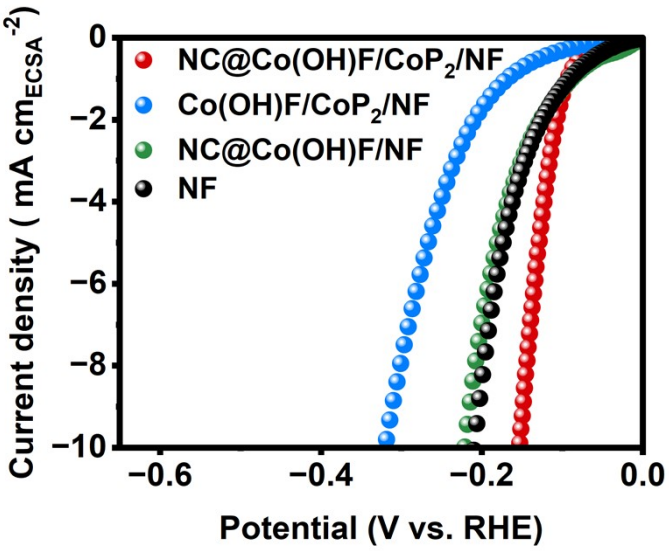

Fig. S8 The ECSA-normalized LSV curves of different electrocatalysts in 1.0 M KOH.

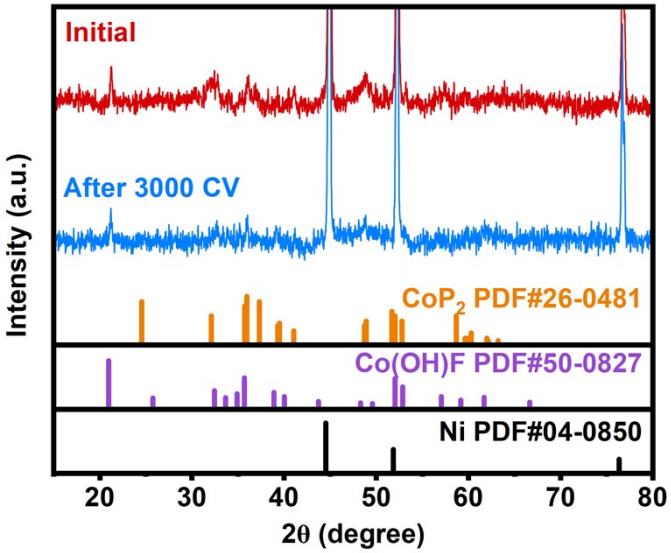

Fig. S9 XRD patterns of NC@Co(OH)F/CoP_2/NF before and after 3000 CV cycles, and the standard PDF cards for CoP_2, Co(OH)F, and Ni.

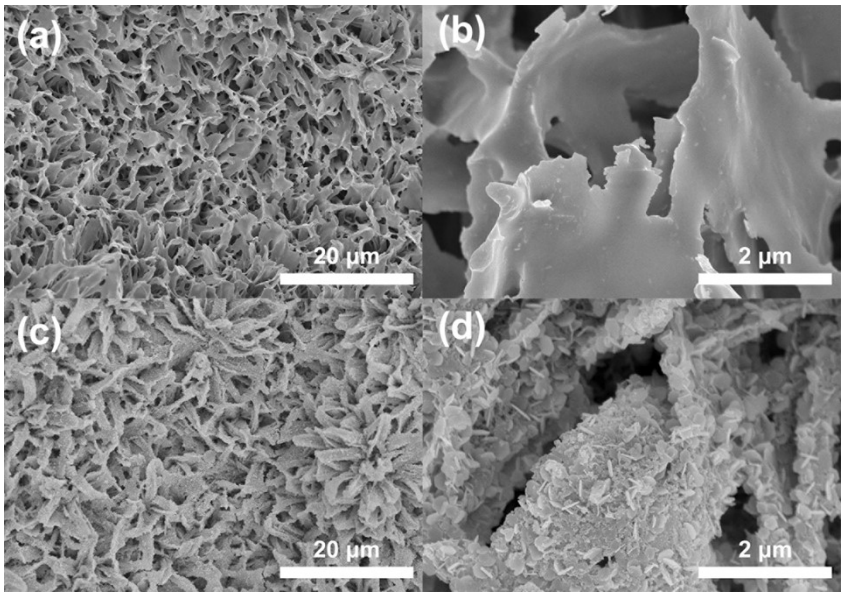

Fig. S10 (a-b) SEM images of NC@Co(OH)F/CoP_2/NF at different magnifications before 3000 HER CV cycles, and (c-d) SEM images of NC@Co(OH)F/CoP_2/NF at different magnifications after 3000 HER CV cycles in 1.0 M KOH.

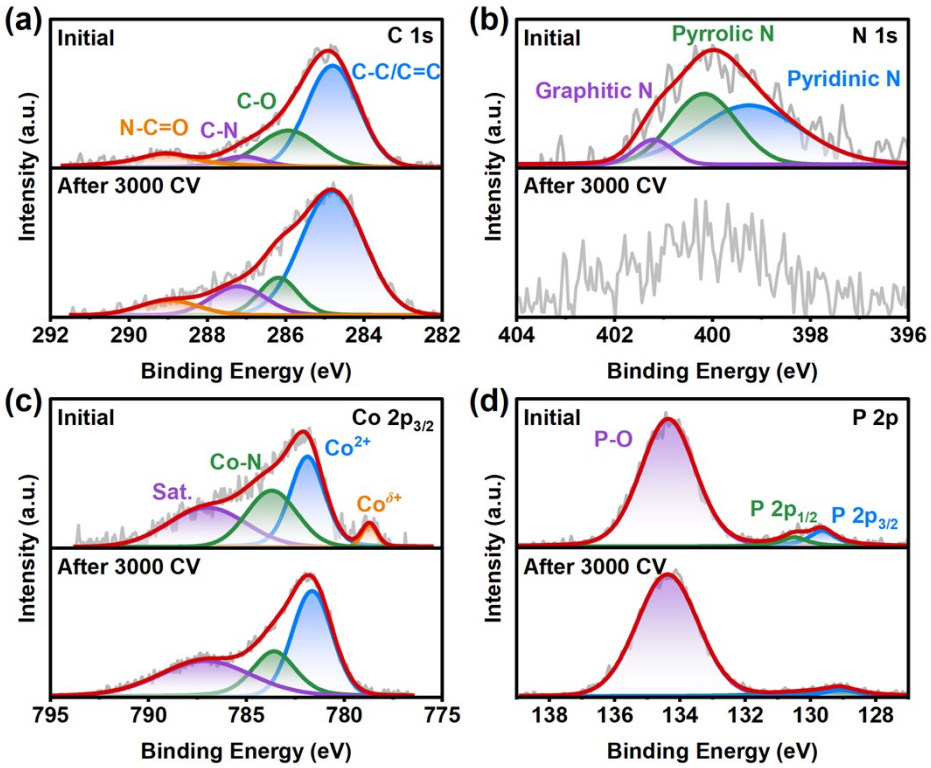

Fig. S11 The comparison of the high-resolution XPS spectra of NC@Co(OH)F/CoP_2/NF before and after HER tests for (a) C 1s, (b) N 1s, (c) Co $2p_{3/2}$, and (d) P 2p, respectively.

Table S1. Comparison of HER performance between NC@Co(OH)F/CoP_2/NF and other nonprecious metal-based HER electrocatalysts in 1.0 M KOH. (*j*: current density; η: overpotential)

Electrocatalyst	*j* (mA cm^{-2})	η (mV)	Ref.
NC@Co(OH)F/CoP_2/NF	100/1000	107/189	This work
CQDs/$Mn_xNi_{5-x}P_4$	100	120	[1]
Vp-CoP-FeP/NF	100	144	[2]
FeP@CoP/NF	100	183	[3]
Fe-CoP	100	227	[4]
NiP/NG	100	300	[5]
FePi-NiS/NF	1000	223	[6]
Te-WSe_2	1000	232	[7]
F-Co_2P/Fe_2P/IF	1000	260	[8]
NiCo@C-NiCoMoO/NF	1000	266	[9]
Ni-Co-P/CFP	1000	295	[10]
NiCoP foam/NF	1000	328	[11]
a-$MoWS_x$/N-RGO	1000	348	[12]
W-$NiCu_{array}$/CM	1000	349	[13]
Mo-NiFeP/NIF	1000	353	[14]
CoP/Cu_2O@CF	1000	358	[15]

Table S2. Comparison of HER performance between NC@Co(OH)F/CoP_2/NF and other nonprecious metal-based HER electrocatalysts in natural seawater containing 1.0 M KOH. (*j*: current density; *η*: overpotential)

Electrocatalyst	*j* (mA cm^{-2})	*η* (mV)	Ref.
NC@Co(OH)F/CoP_2/NF	100/1000	128/237	This work
FeP@CoP/CC	100	220	[16]
$CoMoO_4$/CoP/CC	100	218	[17]
NiFeCr-S/Ni_3S_2/NF	100	236	[18]
Mn-MoWNi	100	261	[19]
NiPS/NF	100	188	[20]
MnCo/NiSe	1000	270	[21]
NiCoHPi@Ni_3N/NF	100	182	[22]
$NiCoP_v$/NF	1000	257	[23]
CoP_x	100	190	[24]
NNNF@Mo_2N/FeOxNy	100	142	[25]
NiFe-P@NC	100	149	[26]

Table S3. ICP test results of the electrolyte after CV cycling test.

Element	Content (mg/L)
Co	0.9
P	216.6

2. Reference

1. W. Chen, Z. Qin, B. McElhenny, F. Zhang, S. Chen, J. Bao, Z. M. Wang, H.-Z. Song and Z. Ren, The effect of carbon quantum dots on the electrocatalytic hydrogen evolution reaction of manganese–nickel phosphide nanosheets, *J. Mater. Chem. A*, 2019, **7**, 21488-21495.

2. L. Qi, Z. Huang, M. Liao, L. Wang, L. Wang, M. Gao, T. Taylor Isimjan and X. Yang, Synergistic Promotion of Large-Current Water Splitting through Interfacial Engineering of Hierarchically Structured CoP-FeP Nanosheets with Rich P Vacancies, *Chem-Eur J*, 2023, **29**, e202301521.

3. C. Lyu, J. Cheng, K. Wu, J. Wu, N. Wang, Z. Guo, P. Hu, W.-M. Lau and J. Zheng, Interfacial electronic structure modulation of CoP nanowires with FeP nanosheets for enhanced hydrogen evolution under alkaline water/seawater electrolytes, *Appl. Catal., B*, 2022, **317**, 121799.

4. L.-M. Cao, Y.-W. Hu, S.-F. Tang, A. Iljin, J.-W. Wang, Z.-M. Zhang and T.-B. Lu, Fe-CoP Electrocatalyst Derived from a Bimetallic Prussian Blue Analogue for Large-Current-Density Oxygen Evolution and Overall Water Splitting, *Adv. Sci.*, 2018, **5**, 1800949.

5. J. Hu, L. Peng, A. Primo, J. Albero and H. García, High-current water electrolysis performance of metal phosphides grafted on porous 3D N-doped graphene prepared without using phosphine, *Cell Rep. Phys. Sci.*, 2022, **3**, 100873.

6. L. Guo, J. Xie, S. Chen, Z. He, Y. Liu, C. Shi, R. Gao, L. Pan, Z.-F. Huang, X. Zhang and J.-J. Zou, Self-supported crystalline-amorphous composites of metal phosphate and NiS for high-performance water electrolysis under industrial conditions, *Appl. Catal., B*, 2024, **340**, 123252.

7. X. Zhang, D. Zhang, X. Chen, D. Zhou, J. Zhang and Z. Wang, Te-doped-WSe_2/W as a stable monolith catalyst for ampere-level current density hydrogen evolution reaction, *Phys. Chem. Chem. Phys.*, 2024, **26**, 3880-3889.

8. X.-Y. Zhang, Y.-R. Zhu, Y. Chen, S.-Y. Dou, X.-Y. Chen, B. Dong, B.-Y. Guo, D.-P. Liu, C.-G. Liu and Y.-M. Chai, Hydrogen evolution under large-current-density

based on fluorine-doped cobalt-iron phosphides, *Chem. Eng. J.*, 2020, **399**, 125831.

9. G. Qian, J. Chen, T. Yu, L. Luo and S. Yin, N-Doped Graphene-Decorated NiCo Alloy Coupled with Mesoporous NiCoMoO Nano-sheet Heterojunction for Enhanced Water Electrolysis Activity at High Current Density, *Nano-Micro Lett.*, 2021, **13**, 77.

10. X. Chen, X. Zhao, Y. Wang, S. Wang, Y. Shang, J. Xu, F. Guo and Y. Zhang, Layered Ni-Co-P Electrode Synthesized by CV Electrodeposition for Hydrogen Evolution at Large Currents, *ChemCatChem*, 2021, **13**, 3619-3627.

11. L. He, Z. Cai, D. Zheng, L. Ouyang, X. He, J. Chen, Y. Li, X. Guo, Q. Liu, L. Li, W. Chu, S. Zhu, X. Sun and B. Tang, Three-dimensional porous NiCoP foam enabled high-performance overall seawater splitting at high current density, *J. Mater. Chem. A*, 2024, **12**, 2680-2684.

12. D. Zhang, F. Wang, W. Zhao, M. Cui, X. Fan, R. Liang, Q. Ou and S. Zhang, Boosting Hydrogen Evolution Reaction Activity of Amorphous Molybdenum Sulfide Under High Currents Via Preferential Electron Filling Induced by Tungsten Doping, *Adv. Sci.*, 2022, **9**, 2202445.

13. K. Wei, H. Hu, Y. Song, Y. Wang, Y. Meng, Y. Wang, J. Zhou and F. Gao, Morphological engineering coupled with electronic engineering accelerates H_2 production at the high current density, *Sep. Purif. Technol.*, 2023, **326**, 124814.

14. Y. Wang, P. Yang, Y. Gong, D. Liu, S. Liu, W. Xiao, Z. Xiao, Z. Li, Z. Wu and L. Wang, Amorphous high-valence Mo-doped NiFeP nanospheres as efficient electrocatalysts for overall water-splitting under large-current density, *Chem. Eng. J.*, 2023, **468**, 143833.

15. R. Qi, X. Liu, H. Bu, X. Niu, X. Ji, J. Ma and H. Gao, In situ growth of phosphorized ZIF-67-derived amorphous CoP/Cu_2O@CF electrocatalyst for efficient hydrogen evolution reaction, *Front. Chem. Sci. Eng.*, 2023, **17**, 1430-1439.

16. K. Zhang, J. Jia, E. Yang, S. Qi, H. Tian, J. Chen, J. Li, Y. Lou and Y. Guo, Work-function-induced electron rearrangement of in-plane FeP@CoP heterojunction enhances all pH range and alkaline seawater hydrogen evolution reaction, *Nano Energy*, 2023, **114**, 108601.

17. X. Yu, P. Xu, Q. Chen, N. Cheng, S. Luo, L. Zhang, B. Zhang and Y. Liu, Built-

in Electric Field of $CoMoO_4$/CoP Heterostructure for Efficient Alkaline Seawater Hydrogen Evolution, *Energy Fuels*, 2024, **38**, 11172-11179.

18. G. Wu, M. Chen, X. Du and X. Zhang, Controlled synthesis of NiFeCr-S/Ni_3S_2 as efficient hydrogen evolution catalyst for seawater splitting and urea splitting, *Fuel*, 2024, **368**, 131660.

19. H. Zhao, M. Liu, X. Du and X. Zhang, Synthesis of polymetallic oxide nanoarrays as efficient hydrogen evolution reaction electrocatalyst for alkaline seawater and urea splitting, *Fuel*, 2024, **372**, 132281.

20. H.-Y. Wang, J.-T. Ren, L. Wang, M.-L. Sun, H.-M. Yang, X.-W. Lv and Z.-Y. Yuan, Synergistically enhanced activity and stability of bifunctional nickel phosphide/sulfide heterointerface electrodes for direct alkaline seawater electrolysis, *J. Energy Chem.*, 2022, **75**, 66-73.

21. R. Andaveh, A. Sabour Rouhaghdam, J. Ai, M. Maleki, K. Wang, A. Seif, G. Barati Darband and J. Li, Boosting the electrocatalytic activity of NiSe by introducing MnCo as an efficient heterostructured electrocatalyst for large-current-density alkaline seawater splitting, *Appl. Catal., B*, 2023, **325**, 122355.

22. H. Sun, J. Sun, Y. Song, Y. Zhang, Y. Qiu, M. Sun, X. Tian, C. Li, Z. Lv and L. Zhang, Nickel–Cobalt Hydrogen Phosphate on Nickel Nitride Supported on Nickel Foam for Alkaline Seawater Electrolysis, *ACS Appl. Mater. Interfaces*, 2022, **14**, 22061-22070.

23. L. Guo, J. Chi, T. Cui, J. Zhu, Y. Xia, H. Guo, J. Lai and L. Wang, Phosphorus Defect Mediated Electron Redistribution to Boost Anion Exchange Membrane-Based Alkaline Seawater Electrolysis, *Adv. Energy Mater.*, **n/a**, 2400975.

24. L. Wu, L. Yu, B. McElhenny, X. Xing, D. Luo, F. Zhang, J. Bao, S. Chen and Z. Ren, Rational design of core-shell-structured CoP_x@FeOOH for efficient seawater electrolysis, *Appl. Catal., B*, 2021, **294**, 120256.

25. Y. He, Y. Hu, Z. Zhu, J. Li, Y. Huang, S. Zhang, M. S. Balogun and Y. Tong, High-performance multidimensional-structured N-doped nickel modulated Mo_2N/FeO_xN_y bifunctional electrocatalysts for efficient alkaline seawater splitting, *Chem. Eng. J.*, 2024, **489**, 151348.

26. Z. Chen, Q. Li, H. Xiang, Y. Wang, P. Yang, C. Dai, H. Zhang, W. Xiao, Z. Wu and L. Wang, Hierarchical porous NiFe-P@NC as an efficient electrocatalyst for alkaline hydrogen production and seawater electrolysis at high current density, *Inorg. Chem. Front.*, 2023, **10**, 1493-1500.